Voltage Profile Improvement in Unbalanced Distribution Networks for Probabilistic Generation and Consumption

Mohammed Bamatraf
Department of Electrical Eng.
Istanbul Technical University
Turkey
matraf21@itu.edu.tr

Oğuzhan Ceylan
Department of Management Information Systems
Kadir Has University, Turkey
oguzhan.ceylan@khas.edu.tr

Ioana Pisica
Department of Electrical and Computer Engineering
Brunel University, London, UK
Ioana.pisica@brunel.ac.uk

Aydoğan Özdemir
Department of Electrical and Electronics Engineering
Kadir Has University, Turkey
Aydogan.ozdemir@khas.edu.tr

***Abstract*—Due to their technical, economical, and environmental advantages, active distribution networks implement renewable energy resources (RERs) such as photovoltaic (PV) units in distribution networks DNs. However, some drawbacks may arise due to the intermittent nature of RERs, such as voltage fluctuations and increased system losses. This paper presents an optimization problem that is solved by sequential linear programming (SLP) to improve the voltage profile of the unbalanced distribution network. A probabilistic approach was applied to both the load profile and the active power generation of the PV units. SLP is applied to the modified IEEE 34 Bus Test system. The method optimizes the voltage deviations by changing the taps of the voltage regulators and the reactive power injected by the inverters of the PV systems and, in some cases, by switching a shunt capacitor. MATLAB simulations are done at different times of the day with different loads and PV outputs to compare base case and optimal case voltage profiles. The results show better voltage profiles after applying the presented approach.**

Keywords— Unbalanced distribution networks, distributed generation, PV systems, sequential linear programming.

I. Introduction

The utilization of (RERs) such as PV systems and WTs is affected by the intermittent and unpredictable nature of their output. Consequently, the poor deployment of such resources into DNs can frequently result in various operational challenges. Some of such are voltage violations, increased active and reactive losses, and unstable frequency. Therefore, it is crucial to implement well-considered control measures before integrating these resources into the DN [1].

Historically, traditional devices like tap regulators and shunt capacitors have long been employed in voltage control and managing the flow of reactive power within the DN. Nevertheless, the growing implementation of RERs has posed a challenge for such conventional devices in improving voltage profiles and power flow. Moreover, recurrent tap switching has a huge impact on the lifespan of such devices [2]. DERs equipped with smart inverters emerge as a promising alternative to enhance voltage control and maintain the voltage stability of the distribution network. This is achieved by offering volt/ var control and decreasing the recurrent use of voltage regulators and capacitors.

Control measures considered before integrating RERs into DNs play a pivotal role in optimizing the efficiency of ADNs. This is achieved by utilizing innovative techniques to facilitate the distributed generation units (DGs) into the DN, which later results in optimal operational performance [3]. Most of the optimization processes in ADNs try to solve optimal power flow equations. Such equations aim to minimize both the operational and generational costs while simultaneously minimizing other objective functions [4].

The authors in [5-7] have addressed the use of heuristic algorithms in solving optimal power flow in distribution networks. The authors in [8-10] discussed nonlinear programming methods. Simple linear programming methods such as interior point and simplex method were used as direct solutions to nonlinear programming problems. Nevertheless, such approaches take longer execution time [11]. Linearizing the nonlinear problem decreases the optimization time. However, the proposed solution may not succeed in finding the optimal point but rather a local optimum; also, convergence problems may occur due to oscillations around a local optimum point [12-14].

The authors in [15] used SLP to solve OPF. The method was effective in terms of convergence, speed, and reliability. The authors in [16] also used SLP to optimize shunt capacitors along with on-load tap changers (OLTC) to control the droop of smart inverters.

This study proposes a faster analytical solution than the heuristic approach and achieves local optimal solutions. SLP aims to improve the voltage profiles by eliminating the voltage violations of undervoltages and overvoltages in unbalanced distributed networks. The proposed method finds the local optimum solutions by changing the reactive power support from the smart inverters of the PV systems and the tap positions of the voltage regulators for each simulation time. The method is implemented on the unbalanced radial distribution feeder IEEE-34 after integrating seven PV units.

In this paper, Section II discusses the problem formulation. Section III presents the test system used in the optimization process. Section IV presents SLP implementation in the optimization problem. Lastly, Sections V and VI show the simulation results and conclusion of the paper.

II. Problem Formulation

The formulation of voltage profile improvement in the unbalanced distribution grid can be represented as a constrained nonlinear optimization problem. The formulation of the optimization problem is presented below.

A. Objective Function (OF)

The objective function here is to minimize all voltage violations, either the overvoltages or the undervoltages, by bringing all the per-phase bus voltages to the allowable limits specified for the distribution networks. The

This article has been accepted for publication in a future proceedings of this conference, but has not been fully edited. Content may change prior to final publication. Citation information: DOI10.1109/PESGM46819.2021.9637910, 2024 18th International Conference on Probabilistic Methods Applied to Power Systems (PMAPS)

mathematical description of the objective functions is presented in (1):

$$OF = \sum_{i=1}^{n} (V_{ref} - V_i)^2 \tag{1}$$

where V_{ref} is the voltage magnitude at the substation, and the V_i is a vector $\boldsymbol{V} = [\boldsymbol{V_1}, \boldsymbol{V_2}, \ldots, \boldsymbol{V_n}]^{\mathbf{T}}$ that represents the voltage magnitudes of feeder busses for all three phases. Note that n is 165 for the IEEE-34 system. It consists of all phases for bus voltages of both original and dummy nodes. Further explanation about the dummy nodes is provided in Sec II.

B. Equality Constraints (EC)

In this study, the equality constraints are the power balance equations. The forward-backward sweep method (FBSM) is used to solve the power flow equations [17]. Equation (2) presents the relationship between the equality constraints, state variables, and decision variables:

$$\boldsymbol{V} = PowerFlow\ [\boldsymbol{X}] \tag{2}$$

where $\boldsymbol{X}$ denotes the control variable vector, consisting of the reactive power output of the smart inverters and the tap positions of the tap-changing transformers. The remaining details of the formulation can be found in [18]

C. Inequality Constraints (IC)

In this study, the inequality constraints are the limits for the system's state variables, i.e., bus voltage magnitude limits and line flow limits. The standard voltage limits in DNs are between 0.95 and 1.05 pu. The inequality constraints are formulated so that it is greater than zero when there is voltage violation (overvoltage or undervoltage) and less than zero when the bus voltages are within the allowable limits as expressed in (3):

$$G_i^j(V_i^j) = \begin{Bmatrix} 0.95 - V_i^j & if\ V_i^j < 0.95 \\ 0 & if\ \ 0.95 \le V_i^j \le 1.05 \\ V_i^j - 1.05 & V_i^j > 1.05 \end{Bmatrix} \tag{3}$$

In (3), i and j refer to the bus number, including all phases and the time step, respectively. The inequality constraint for each time step -j is expressed as follows:

$$\mathrm{G}^j(\mathbf{V}) = \sum_{i=1}^{n} G_i^j(V_i^j) \tag{4}$$

The final expression of the constrained optimization problem at simulation time-j can be given as follows:

$$\begin{aligned} Minimize \quad & OF = \sum_{i=1}^{n} (V_{ref} - V_i^j)^2 \\ Subject\ to \quad & \boldsymbol{V^j} = PowerFlow\ [\boldsymbol{X^j}] \\ & \mathrm{G}^j(\mathbf{V}) \le 0 \end{aligned} \tag{5}$$

D. Control Variables (CV)

Three types of decision variables are considered and optimized to achieve the best voltage profile for each simulation time.

1) Reactive power support from PV units (smart inverter)

All photovoltaic systems have inverters that function as DC-AC converters. New PV systems have smart inverters that also allow for reactive power flow from the PV system to the DN and vice versa. The decision variables for the inverter are expressed as the three-valued vector in (6). Note that the smart inverter of the PV system can only provide reactive support when there is some active power generation. In this study, it is assumed that the active power generation from the PV must at least be 5% of the rated power to allow for reactive power support.

$$Q = [Q_a\ Q_b\ Q_c]^T = [X_1\ X_2\ X_3]^T \tag{6}$$

The phase reactive powers (Q_a , Q_b, and Q_c) are assumed to be between -90 kVAr and 90 kVAr because of the PV capacity. Moreover, equation (7) also constrains the amount of reactive power that is to be provided by the PV. The available reactive power follows the same pattern as the active power during the day.

$$Q = \sqrt{S^2 - P^2} \tag{7}$$

2) Tap positions of the voltage regulators

The IEEE-34 system is equipped with two voltage regulators located between 814-850 and 832-854. The decision variable of the tap regulators is a fixed integer value between [-16, 16]. One tap action contributes to a change of 0.00625 pu. Note that the decision variable here is a discrete value, which makes the optimization problem a mixed-integer.

$$T_1 = [X_{22}\ X_{23}\ X_{24}]^T\ T_2 = [X_{25}\ X_{26}\ X_{27}]^T \tag{8}$$

3) Shunt Capacitor

This regulating device is only used in an emergency when the reactive power support from the other alternatives, i.e., smart inverters and tap changers, is insufficient to fix the undervoltage violations at node 890. This happens at 10:00 a.m. and 3:45 p.m. when there is no sufficient active power generation, as shown in Fig. 3. The power rating of the capacitor is 50 kVAr.

III. Test System

A. IEEE 34 Node Test Feeder

The IEEE 34-System is a radial distributed network used for distributed generation studies [19]. The configuration of the 34 system, along with the modifications of integrated PV units and their locations, are shown in Fig. 1.

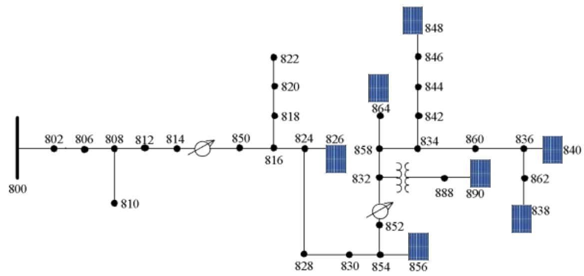

Fig. 1. IEEE-34 node test feeder and locations of PV units.

B. High PV penetration

Seven PVs are integrated into the DN, each with a power rating of 90 kW. These units were allocated during the planning (design) phase with respect to the voltage and load levels at the nodes. In this regard, they are distributed at nodes far from the upstream network and supply greater loads. Note that if the PV systems are distributed along the DN, it would result in a more efficient PV penetration [20]. However, overvoltage problems may arise during high solar irradiation times.

This article has been accepted for publication in a future proceedings of this conference, but has not been fully edited. Content may change prior to final publication.
Citation information: DOI10.1109/PMAPS61648.2024.10667300, 2024 18th International Conference on Probabilistic Methods Applied to Power Systems (PMAPS)

C. *Load profile*

The original test system has 99 load buses (3*33). However, there are some distributed loads between some buses. In order to account for such loads, new buses are created at the middle point of the two buses to carry half of the distributed load, and the other half is passed on to the next bus. This resulted in a total number of 55 nodes instead of 33. Both the spot loads and the distributed loads are consistent with those provided in the datasheet for the IEEE-34 node test feeder in [19].

All bus nodes follow the load profile depicted in Fig. 2 [21]. Since there is a reassumed unpredictability for all loads, a 10% random deviation of the recorded data is applied to all nodes at every simulation time.

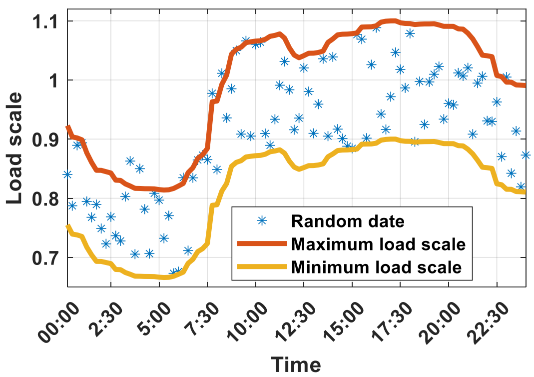

Fig. 2. Scaled load pattern for the distribution system.

D. *Photovoltaic Units*

Fig. 3 shows the active power output for the 90 kW PV units. The data is retrieved at a 15-minute resolution. This profile is modified from the original data retrieved from [22] and shows active power generation for an ideal day. Uniform random variation was applied to depict a generally random day with all possible scenarios. The resulting characteristics show very fast-changing radiation (output power).

Equation (9) shows the constraints for the reactive power, which consists of the power factor and power rating. Fig. 3 Shows both the resulting active power generation after applying random output and the corresponding available reactive power for each time step.

$$Q = Min\{\sqrt{S^2 - P^2}, P * \tan(\emptyset)\} \quad \emptyset = cos^{-1}0.95 \tag{9}$$

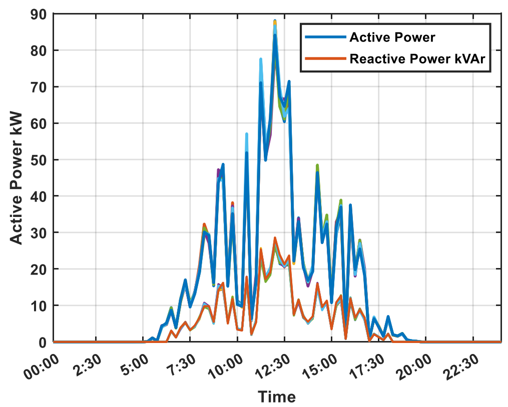

Fig. 3. PV output power and available reactive power with a minimum of 0.95 power factor.

IV. Implementation of SLP Optimization

SLP method is quite practical when it comes to solving nonlinear optimization problems. The method starts by choosing an operational point and then linearizing the objective function and the inequality constraints around it. After formulating the linearized problem, the simplex method is used to solve the linearized problem. The decision variables consist of the support of the reactive power provided by the PV units and the tap positions of the voltage regulators:

$$X = [Q^T \; T_1^T \; T_2^T C] \tag{10}$$

$$Q^T = [X_1, \dots, X_{21}]^T \tag{11}$$

$$T_1 = [X_{22} \; X_{23} \; X_{24}]^T \; T_2 = [X_{25} \; X_{26} \; X_{27}]^T \tag{12}$$

$$C = X_{28} \text{ Where } X \text{ is either 0 or 1} \tag{13}$$

The per-phase bus voltages are the state variables to be optimized to their allowable limits.

$$\boldsymbol{V_{min}} \leq \boldsymbol{V} = [V_1 \; V_2 \dots V_{165}]^T \leq \boldsymbol{V_{max}} \tag{14}$$

Here, $\boldsymbol{V_{min}}$ and $\boldsymbol{V_{max}}$ are 165*1 vectors, whose entries are the minimum and maximum voltage magnitudes, i.e., 0.95 p.u. and 1.05 p.u., respectively. A detailed explanation of the optimization process for the SLP is presented below [23].

Step-1 The SLP optimization process starts by choosing an operational point x_0 and linearizing the objective function $F(x)$ around it, which yields the following linearized objective function;

$$\tilde{F}(\boldsymbol{X}) = F(\boldsymbol{X}_0) + \nabla F(X_0)^T * \boldsymbol{X} \tag{15}$$

The term ∇ here refers to the gradient operator.
Step-2 The linearization process then comes to the inequality function $G(x)$ and the yields the following linearized inequality constraint

$$\tilde{G}(\boldsymbol{X}) = G(\boldsymbol{X}_0) + \nabla G(X_0)^T * \boldsymbol{X} \tag{16}$$

Step-3 After obtaining two linearized functions, any basic linear optimization technique can be used to solve the optimization problem in Eq. (17). In this study, the simplex method is used.

$$\begin{aligned} &Minimize \; \tilde{F}(\boldsymbol{X}) \\ &Subject \; to \; \tilde{G}(\boldsymbol{X}) \leq 0 \end{aligned} \tag{17}$$

Step-4 After finding the solution for Eq. (17), the initial operational point is updated as expressed in Eq. (18)

$$\boldsymbol{X}_{new} = \boldsymbol{X}_0 + \boldsymbol{X}_{sol} \tag{18}$$

Step-5 Starting from step 2, the process is repeated until one of the following two criteria is satisfied.

$$|\boldsymbol{X}_{new} - \boldsymbol{X}_{old}| \leq \in or \; |F(x_{new}) - F(x_0)| \leq \in \tag{19}$$

∈ Refers to a chosen tolerance value of 0.0001.

This article has been accepted for publication in a future proceedings of this conference, but has not been fully edited. Content may change prior to final publication.
Citation information: DOI10.1109/PMAPS61648.2024.10667300, 2024 18th International Conference on Probabilistic Methods Applied to Power Systems (PMAPS)

V. Simulation Results

MATLAB is used as a computation tool. The voltage magnitudes for the base case operation where there isn't any reactive power and voltage control (no reactive power support from PV units and capacitors, and all tap positions are at zero) are illustrated in Fig. 4. Different colors in the figure show different simulation times. Note that there are 165 per-phase voltages that were plotted, but only a few were labeled on the x-axis of the figures for visual clarity. There are some undervoltage problems on some buses. The same bus voltage magnitudes are illustrated in Fig.5 for uncontrolled high PV penetration cases where there is no reactive power support from PV units and the tap positions are still 0. One can realize that the undervoltage violation levels are decreased in this case but not eliminated because of a lack of reactive power support. Moreover, there are additional overvoltage problems at some hours due to high PV penetrations.

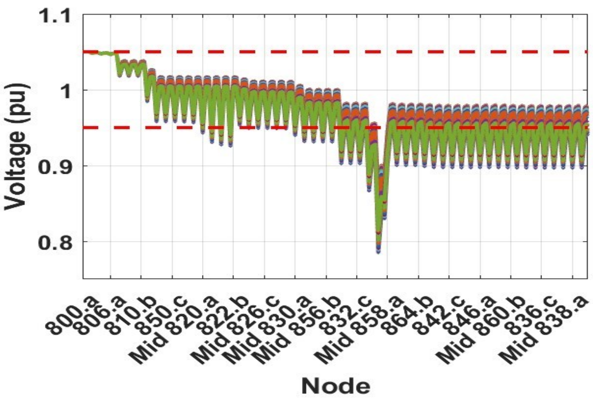

Fig. 4. Base case voltage profiles for 24 hours.

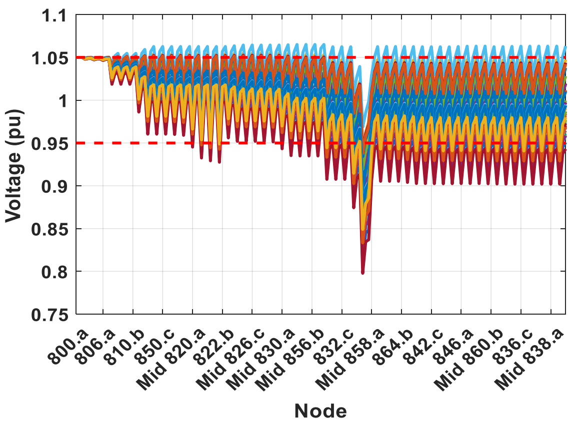

Fig. 5. Voltage profiles for 24 hours after high PV penetration.

SLP is used to solve Eq. (5) to eliminate the severe undervoltage problems at node 890 that occur in the morning and later during the daytime. SLP is also used to eliminate the overvoltage violations that take place during high solar irradiation times. Some representative hours are considered to show the performance of SLP to improve the voltage profiles at such times.

A. *Simulation results at 12 a.m.*

Fig. 6 shows the simulation results after using SLP. The PVs are inactive, and the load is relatively low at this hour. Since there is available reactive power at such time, only tap positions are optimized to improve the voltage profile. This similar behavior of eliminating the undervoltage violations using only tap positions is valid for the inactive PV and low load conditions up to 6:30 a.m.

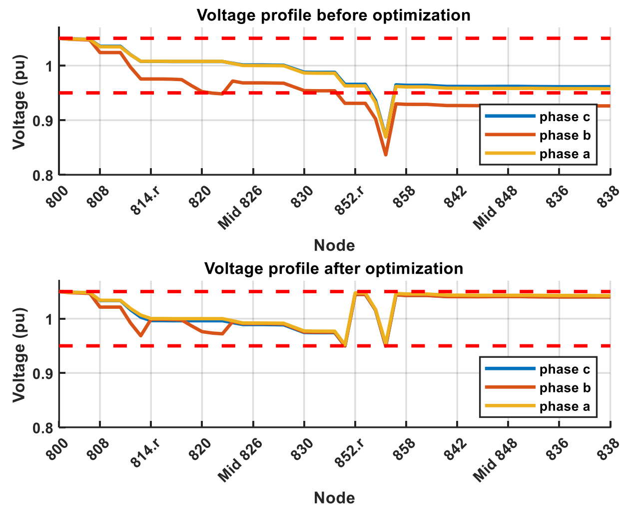

Fig. 6. Base case and optimal voltage profiles at 12 a.m.

B. *Simulation results at 9 a.m.*

At this time, the load starts to increase, and the available control variables are the limited reactive power support from the PV units and the voltage regulators. Fig. 7 shows the voltage profiles where the undervoltage problems at node 890 are eliminated by changing the tap positions and providing reactive power support from the PV. This behavior continues all day except for a few critical time slots when the active power generation drops drastically.

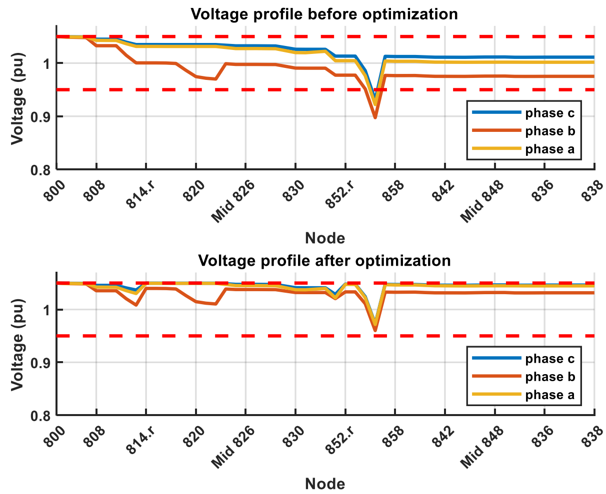

Fig. 7. Base case and optimal voltage profiles at 9 a.m.

C. *Simulation results at 10:00 a.m.*

At this time, the load is still increasing. However, there is a sudden decrease in PV active/reactive power, probably because of shading. The reactive power support from the smart inverter and controlling the tap positions are insufficient to fix the undervoltage problem at node 890. Therefore, the shunt capacitor at node 890 is switched on to maintain the desired voltage magnitude level. The results are depicted in Fig. 8. Similar behavior and corrective action are applicable to a few critical times, as shown in Fig. 9 at 3:00 p.m. and 3:45 p.m.

This article has been accepted for publication in a future proceedings of this conference, but has not been fully edited. Content may change prior to final publication. Citation information: DOI10.1109/PMAPS61648.2024.10667300, 2024 18th International Conference on Probabilistic Methods Applied to Power Systems (PMAPS)

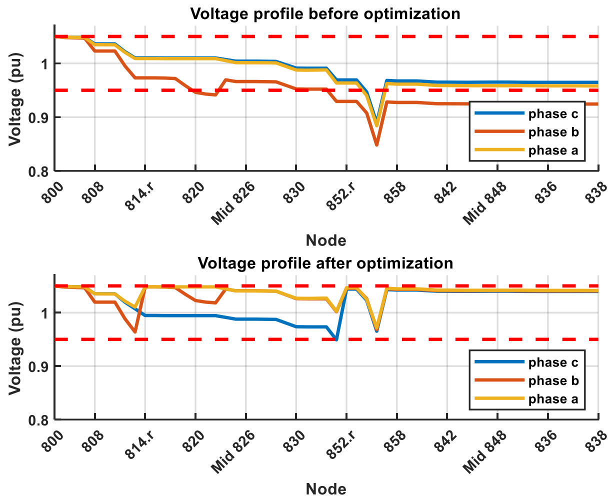

Fig. 8. Base case and optimal voltage profiles at 10:00 a.m.

D. All Daytime Simulations.

Fig. 9 shows all the voltage profiles for all phases from 12:00 a.m. to 4:30 p.m. There are some slight undervoltage problems at some hours.

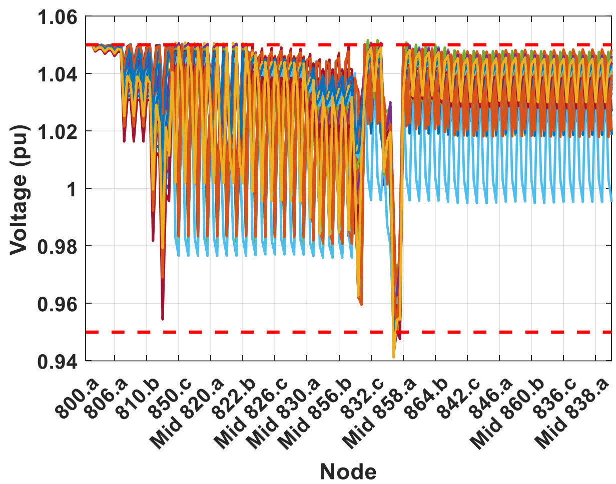

Fig. 9. All profiles after optimization from 12:00 a.m. to 4:30 p.m.

E. Reactive Power from inverters.

Fig. 10 presents the optimal combinations of the reactive power support to be provided by the smart inverter of the PV units. Note that the reactive power support starts right after 6:30 a.m., but the maximum support follows the pattern of the active power generation in Fig. 3. Moreover, there are sudden switching between charging and discharging states due to the fast-changing characteristics shown in Fig. 3.

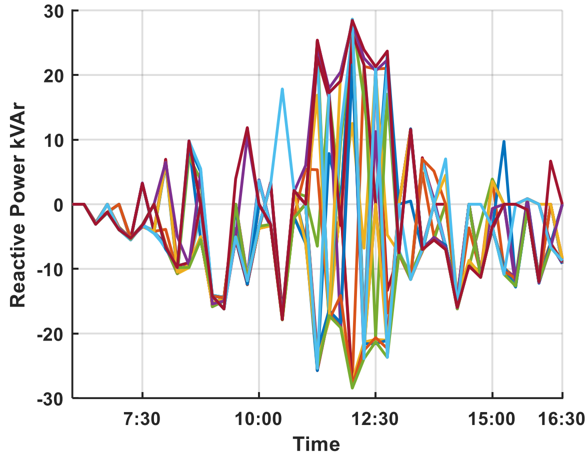

Fig. 10. Reactive power support of the smart inverters.

F. Voltage Regulators and Capacitor state

Fig. 11 shows optimal tap positions and the capacitor state during optimization. Note that the number of tap actions is high because of the active power profile fluctuation, making it harder to solve the undervoltage problems without resorting to the regulators and the capacitor. The overall time of using the reactive support from the capacitor was about 3 hours, as shown in Fig 13.

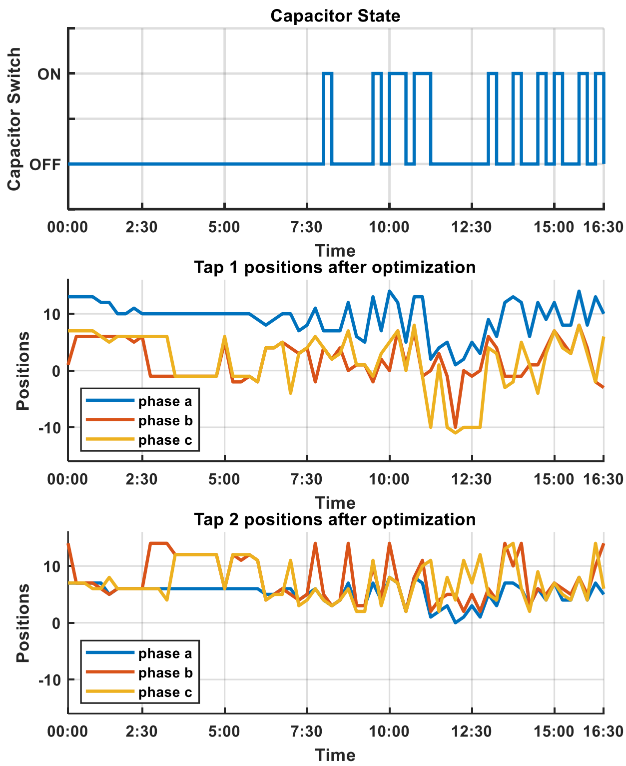

Fig. 11. Optimal tap positions of regulators and capacitor state along the day.

VI. Conclusions

This paper has proposed a classical and analytical optimization method to improve voltage profiles in unbalanced DNs. The proposed method controls both the voltage regulators and the reactive power support from the smart inverters of the multiple PV systems and, at critical times, utilizes a shunt capacitor when the other options are insufficient to achieve the intended goal. SLP was implemented to solve the optimization problem at each time step. The proposed approach was implemented on the IEEE 34-node test feeder after integrating 7 PV units.

The simulation results demonstrate that using SLP has effectively improved and brought the voltage profiles to the permissible limits from 12 a.m. in the morning to 4:30 p.m. in the afternoon. During times when active power generation is absent, the voltage regulators were sufficient to control and fix the undervoltage problems at node 890. The results also show that the integration of multiple PV units into different locations of the DN contributes significantly to improving the voltage violations at the corresponding node by providing the necessary reactive power support (injecting) for undervoltages and (consuming) for overvoltages without the expected increase in the reactive power losses on the lines.

However, fast-changing PV output profiles made it challenging to solve the voltage violations using only the reactive power support. From 8:30 a.m. to 4:30 p.m., all three control variables contributed to the optimization process. This led to the one and repeated tap actions during the fast-changing active power generation.

The proposed method shows that the changes in the suggested control variables guarantee a more efficient and reliable operational performance for the distribution network. The execution time for every time step simulation lasts between five to sixteen seconds. This is a good number, and it makes it eligible for online strategies in ADNs.

Acknowledgment

This research is funded as a part of the "120N996 Implementing digitalization to improve energy efficiency and renewable energy deployment in Turkish distribution networks" project under the framework of the 2551 Project organized by TUBITAK and the British Council.

References

[1] Adajah, Yisah Y., et al. "Distributed Generation (DG): A Review." *2021 1st International Conference on Multidisciplinary Engineering and Applied Science (ICMEAS)*. IEEE, 2021.

[2] Spertino, Filippo, et al. "Voltage control in low voltage grids with independent operation of on-load tap changer and distributed photovoltaic inverters." *Electric Power Systems Research* 211 (2022): 108187.

[3] Guerrero, Jaysson, et al. "Towards a transactive energy system for integration of distributed energy resources: Home energy management, distributed optimal power flow, and peer-to-peer energy trading." Renewable and Sustainable Energy Reviews 132 (2020): 110000.

[4] Kou, Peng, et al. "Safe deep reinforcement learning-based constrained optimal control scheme for active distribution networks." *Applied Energy* 264 (2020): 114772.

[5] Ahmadi, B., Ceylan, O., Ozdemir, A., "Distributed energy resource allocation using multi-objective grasshopper optimization algorithm," Electric Power Systems Research, Volume 201, Article Number107564. 2021.

[6] Ahmadi, B., Ceylan, O., Ozdemir, A., Fotuhi-Firuzabad, M., "A multi-objective framework for distributed energy resources planning and storage management," Applied Energy, 314(1):118887, May 2022.

[7] Ahmadi B, Ceylan O, Ozdemir A. A multi-objective optimization evaluation framework for integration of distributed energy resources. J Energy Storage 2021; 41:103005.

[8] Montoya, O. D., et al. "A mixed-integer nonlinear programming model for optimal reconfiguration of DC distribution feeders." *Energies* 13.17 (2020): 4440.

[9] Zhang, Yanqi, et al. "Research on logistics management layout optimization and real-time application based on nonlinear programming." *Nonlinear Engineering* 10.1 (2022): 526-534.

[10] Pirouzi, Sasan, Mohammad Amin Latify, and G. Reza Yousefi. "Conjugate active and reactive power management in a smart distribution network through electric vehicles: A mixed integer-linear programming model." *Sustainable Energy, Grids and Networks* 22 (2020): 100344.

[11] G. Liu, O. Ceylan, Y. Xu, and K. Tomsovic, "Optimal voltage regulation for unbalanced distribution networks considering distributed energy resources," 2015 IEEE Power & Energy Society General Meeting, Denver, CO, USA, 2015, pp. 1-5, doi: 10.1109/PESGM.2015.7286473.

[12] Mhanna, Sleiman, and Pierluigi Mancarella. "An exact sequential linear programming algorithm for the optimal power flow problem." *IEEE Transactions on Power Systems* 37.1 (2021): 666-679.

[13] Girigoudar, Kshitij, and Line A. Roald. "Linearized three-phase optimal power flow models for distribution grids with voltage unbalance." *2021 60th IEEE Conference on Decision and Control (CDC)*. IEEE, 2021.

[14] Yang, Tianshu, et al. "A linear branch flow model for radial distribution networks and its application to reactive power optimization and network reconfiguration." *IEEE Transactions on Smart Grid* 12.3 (2020): 2027-2036.

[15] Ilunga, Gad, and AP Sakis Meliopoulos. "A Convex Solution-Sequential Linear Programming Methodology for the Quadratized-OPF Problem." *2023 IEEE Power & Energy Society General Meeting (PESGM)*. IEEE, 2023.

[16] Dubravac, Marina, et al. "Voltage Optimization in PV-Rich Distribution Networks—A Review." *Applied Sciences* 12.23 (2022): 12426.

[17] Abdelwareth, Mohamed Els S., Dedet Candra Riawan, and Chow Chompoo-inwai. "Optimum Generated Power with the Minimum Cost of a Radial Network using Firefly and Genetic Algorithms." *2021 International Conference on Power, Energy and Innovations (ICPEI)*. IEEE, 2021.

[18] Bamatraf, M., Ceylan, O., Pisica, I., Ozdemir, A., "SLP Optimization-Based Method to Improve Voltage Profiles in Unbalanced Distribution Networks", 6th International Conference on Smart Energy Systems and Technologies – SEST 2023, 4-6 September, 2023, Mugla-TURKEY

[19] IEEE 34 Node TestFeeder. "Distribution System Analysis Subcommittee Report." IEEE Transactions, 2003.

[20] O. Ceylan, S. Paudyal, B. Bhattarai and K. Myers, ”Photovoltaic Hosting Capacity of Feeders with Reactive Power Control and Tap Changers”, 2017 IEEE PES Innovative Smart Grid Technologies Conference Europe (ISGT-Europe), 2017.

[21] https://seffaflik.epias.com.tr/transparency/

[22] https://ideas.repec.org/a/eee/energy/v114y2016icp1251-1265.html.

[23] Venkataraman, P., 2009. Applied Optimization with MATLAB Programming, second ed. John Wiley and Sons, Hoboke